4th International Conference on the Durability of Concrete Structures
24–26 July 2014
Purdue University, West Lafayette, Indiana, USA

Comparative Study of Alkali-Activated Fly Ash Manufactured Under Pulsed Microwave Curing and Thermal Oven Curing

S. Shi and Y. Bai
Department of Civil, Environmental and Geomatic Engineering, University College London, U.K.

H. Li and D. L. Xu
Institute of Powder Engineering, Xi'an University of Architecture and Technology, P.R. China

P. A. M. Basheer
School of Planning, Architecture and Civil Engineering, Queen's University Belfast, U.K.

ABSTRACT

This paper compares the alkali-activated fly ash (AAFA) manufactured with thermal oven curing and pulsed microwave curing methods. Fly ash activated by 8M NaOH solution at a liquid to solid ratio of 0.3 was cured by thermal oven at 85°C and domestic microwave oven, respectively. Apart from compressive strength test, the temperature profiles of AAFA samples were captured by thermal camera. Reaction products of AAFA were characterised with XRD, FTIR and TG/DTG, while the microstructure of AAFA was analysed by MIP and SEM. The results showed that with much shorter curing duration, the compressive strength of AAFA samples under microwave curing was comparable to those samples under thermal oven curing. The XRD results demonstrated that different reaction products were generated from thermal oven curing (hydroxysodalite) and microwave curing (chabazite-Na) respectively. The FTIR spectra showed that aluminosilicate with higher degree of polymerization was formed in the sample with microwave curing. MIP indicated equivalent total porosities from both curing methods, while a well-distributed matrix phase under thermal oven curing were found in the SEM results. Overall, the results demonstrate that microwave curing has great potential to be an alternative curing method for manufacturing AAFA.

Keywords: alkali-activated fly ash, pulsed microwave curing, thermal oven curing.

1. INTRODUCTION

Portland cement (PC), the most widely used construction material in the world, contributes to about 5% of CO_2 produced by mankind annually (Fonta, 2013). Therefore, enormous efforts have been made to develop eco-friendly construction materials in order to reduce the CO_2 emission. In the same vain, fly ash, a by-product from coal power plant, is produced on a large scale each year. More than 65% of fly ash is stockpiled at coal power plants or disposed of in landfills, which can impact negatively on the environment. Therefore, how to recycle fly ash more effectively has received increased attention. Although fly ash has been used as an addition in blended cements to replace part of the Portland cement, such as CEM II and CEM IV in the current European standard, at high replacement levels the early-age strength of concrete is usually low (Felekoglu, 2006; Durán-Herrera et al., 2011), which has caused concerns in industrial applications.

Since fly ash is rich in alumina and silica, it could also be activated directly by alkaline solution without using any PC to produce a non-clinker cementitious material, alkali-activated fly ash (AAFA). Due to its environmental friendly nature, AAFA has been considered as a potential alternative to replace PC in certain industrial applications (Bakharev, 2005b; Palomo et al., 1999; Miranda et al., 2005). It has been proposed that the reaction process of AAFA is a chemical process which involves two main stages, namely, dissolution and polymerization (Fernández-Jiménez et al., 2005). In the dissolution stage, the reactive silica and alumina components in fly ash are dissolved under strong alkaline condition (Bakharev, 2005b), whilst in the polymerization stage, the dissolved reactive silica and alumina polymerize to produce the main reaction product, sodium aluminosilicate hydrate along with a small quantity of zeolites (Palomo et al., 1999), leading to the formation of a well-compacted cementitous binding material. Compared to PC system, it has been claimed that AAFA produces lower CO_2 emission, consumes less energy and possesses superior durability (Bakharev, 2005a; Miranda et al., 2005;

Fernandez-Jimenez et al., 2006). However, the strength development of AAFA is very slow under room temperature and thermal curing has been considered essential for the initiation of the chemical reaction and subsequent strength development (Puertas et al., 2003; Katz, 1998; Criado et al., 2005). Currently, the prevailing curing method for AAFA is thermal curing in an oven at 85^{o}C, which, depending on the reactivity of fly ash, normally takes more than 8 hours to obtain an early strength of above 20 MPa (Criado et al., 2005). However, the main drawback of thermal oven curing is that it inevitably increases the energy consumption, offsetting the benefits which can be obtained from AAFA.

Compared to conventional thermal heating, such as thermal oven, it is generally agreed that microwave is a low energy heating source. The dominant heating mechanism in thermal oven curing is thermal radiation and conduction, whereby the heat is conducted from the surface to the core of the samples, which is not only slow, but also generates thermal gradient throughout the sample. Consequently, it can potentially lead to thermal cracks, affecting the strength development. In contrast, microwave heating is a more effective method, in particular, for heating up dielectric materials. As all the components in concrete, such as water, cement and aggregate are dielectric materials, concrete itself can be considered as a dielectric material (Metaxas & Meredith, 1983). Water, in particular, is a good dielectric material. Under the alternating electromagnetic field of microwave, the dipolar molecules of these dielectric materials can vibrate and, thus, generate frictions between the molecules which then convert microwave energy into heat energy instantly and volumetrically (Metaxas & Meredith, 1983). Thus, the curing duration and energy consumption of microwave heating can be reduced dramatically.

In the past, many investigations have been conducted into the potential of using microwave as an accelerated curing technique for PC-based concrete. For example, Wu et al. (Wu et al., 1987) used a domestic microwave oven (full power of 650W) to cure mortar samples (4×4×16cm) manufactured with Type I OPC (as per ASTM C150) immediately after casting. Their results indicated that compressive strength around 60 MPa could be achieved within 30 minutes at 150W. However, at higher power level the cement slurry splashed out possibly due to the violent evaporation of water. To avoid this, Hutchison et al. (R. G. Hutchison et al., 1991) introduced water load (i.e. extra water) into a domestic microwave oven when they cured a Type I OPC mortar (4×4×16cm) immediately after casting. It was found that part of the microwave power could be absorbed by this water load and, as a result, the splash of the cement slurry was avoided. In another study, Leung and Peeraphan (1997, 1995) reported that a 30-min delay (i.e., presetting time before microwave curing) could improve the strength development of the mortar and concrete samples manufactured with Type III OPC (ASTM C150).

Rattanadecho et al. (2008) applied a microwave continuous belt drier to cure Type I OPC paste (5×5×5cm) with a delay time of 24 hours. The development of the early compressive strength could be accelerated by microwave curing. It was found that after microwave curing for 15 min and 30 min, the strength of the cement samples with microwave curing method reached a plateau after 7 days, while the strength decreased slightly after 28 days.

Furthermore, contrary to some commonly held belief, previous modelling results and experimental study all confirmed that the temperature was not uniformly distributed in the microwave cured samples (Makul et al., 2010; Knoerzer et al., 2008). Nonetheless, based on the previous research on curing PC-based products, it can be clearly seen that microwave curing can greatly reduce the curing duration. However, at the high power level, it would lead to splashing and cracks due to overheating inside the samples as observed in the previous studies (Wu et al., 1987; R. G. Hutchison et al., 1991).

Despite many investigations into the use of microwave to cure PC-based concrete products, the research on curing AAFA with microwave curing is scarce. The only study reported in the literature was carried out by Somaratna et al. (Somaratna et al., 2010) on curing AAFA mortars (5×5×5cm) with a domestic oven. With a delay time of 12 hours, the mortars were cured with different curing durations at varying percentages of full power level. It was noticed that high percentages of full microwave power (30%, 60% and 100%) caused severe crack inside the sample, possibly due to the evaporation of water and overheating and, hence, uneven temperature distribution inside the sample. After microwave heating, the temperature difference between the core and the surface of the sample was found to be up to 35^{o}C. Moreover, the temperature of the sample reached 140^{o}C or even above 210^{o}C, which would be harmful to the strength development. Nonetheless, the compressive strength of AAFA samples with microwave curing for 120 min was found to be higher than that with thermal oven curing at 75^{o}C for 48 hours, indicating a good potential of microwave curing for manufacturing AAFA products.

To solve the uneven temperature distribution during microwave heating process, the pulsed microwave heating (Gunasekaran & Yang, 2007a, 2007b), has been widely employed in food industry. A typical pulsed microwave heating regime usually consists of 'power-on' and 'power-off' duty cycles. The overall idea is to use the 'power-off' period to allow the heat to be transferred from high temperature region to the low temperature region through thermal conduction so that, not only an even temperature distribution could be achieved, but also the energy consumption could be reduced. However, the 'pulsed' microwave concept has not been attempted by cement and concrete researchers. Therefore, this paper is mainly focused on investigating the potential of using pulsed microwave technique for manufacturing AAFA material. The water load and delay time concept as established by previous researchers in the literature are also considered in order to optimize the microwave curing regime for AAFA systems. The mechanical performance, temperature profile, hydration products and microstructure of AAFA material manufactured with different pulsed microwave curing regimes were characterized and then compared with those of the AAFA products manufactured with thermal oven curing.

2. EXPERIMENTAL

2.1 Materials

The fly ash used in this work was supplied by Weihe coal power plant, Shaanxi, China. The chemical composition of the fly ash is as follows: SiO_2 – 49.29%, Al_2O_3 – 30.55%, Fe_2O_3 – 5.55%, CaO – 5.96%, MgO – 0.81%, Na_2O – 0.74%, K_2O – 1.38%, SO_3 – 0.63%, Ti_2O - 1.08%, and LOI – 1.87%. The particle size distribution of the fly ash is shown in Fig. 1. Sodium Hydroxide of industrial grade with a purity of 95% was supplied by ReAgent.

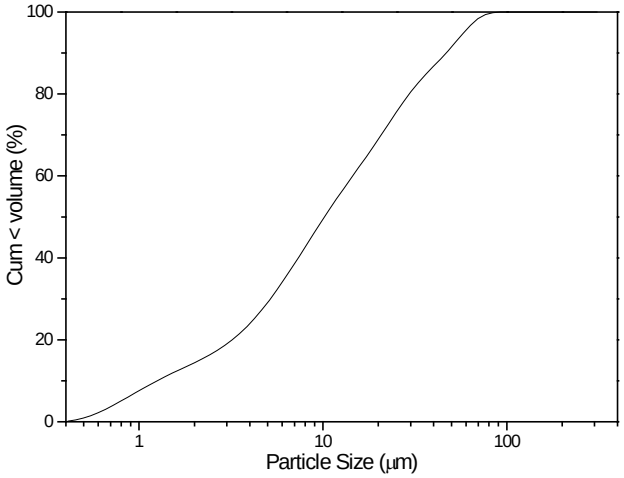

Figure1. The particle size distribution of raw fly ash.

2.2 Preparation of samples

The AAFA paste was produced by mixing the fly ash with 8M NaOH solution at solution to solid ratio of 0.3. The fresh paste was cast into four three-gang steel moulds for thermal oven curing and four three-gang PEEK moulds for microwave curing respectively. The dimension of the samples was 25mm by 25mm by 25mm. The samples were then cured under thermal curing at 85^{o}C and pulsed microwave curing as described in detail below:

- ***Thermal oven curing at 85^{o}C***: In this study, the thermal oven curing at 85^{o}C was employed as control since this curing regime is the most established in the literature. Furthermore, in both thermal oven and microwave curing, a 24-hour room temperature pre-curing regime was adopted, which will not only reduce slurry splashing in microwave curing (Somaratna et al., 2010), but would also enhance the dissolution of silica and alumina from fly ash, leading to better activation (Bakharev, 2005b). The pre-cured samples were cured within steel moulds under room temperature for 24 hours before being exposed to the thermal oven curing up to 24 hours.

- ***Pulsed microwave curing***: Similar to the thermal oven curing, prior to the curing in a domestic microwave oven, AAFA samples were pre-cured at room temperature for 24 hours. The pulsed microwave curing regime used in this study was achieved through the control of 'power-on' and 'power-off' duty cycles during the microwave curing process, which was operated by setting the value of pulsing ratio (PR) as defined below:

$$PR = \frac{t_{on}}{(t_{on} + t_{off})}$$

where, t_{on} and t_{off} are the 'power-on' and 'power-off' durations of the microwave pulses per duty cycle respectively. The pulsing ratio was 0.05 and each cycle lasted for 2 min in this study. A water load of 200g was applied.

Following thermal oven curing and microwave curing, all the samples were cooled down to room temperature prior to the compression test. Selected debris from the compression tests was soaked in acetone for three days in order to arrest further reaction. The debris was then filtered to remove the acetone before being stored in the desiccator under vacuum for another three days. After this, some of the debris was partly ground into fine powder and the particles passed 63μm sieve was used for further chemical analysis. The rest of the debris was well kept for further microstructures analysis.

2.3 Analysis techniques

The compressive strength of the AAFA samples was tested after 2 hours, 4 hours, 7 hours and 24 hours under thermal oven curing and after 10 cycles, 20 cycles, 30 cycles and 40 cycles under microwave curing, respectively.

The temperature profile of the cross section of each sample was captured by a FLIR E60bx thermal camera on the fractured surface immediately after the AAFA samples were split into two halves using a tailor designed moulds after each thermal oven curing and microwave curing were completed.

Reaction products were characterised by means of X-ray Diffraction (XRD), Fourier Transform Infrared Spectroscopy (FTIR), Thermogravimetric and Differential Thermogravimetric (TG/DTG) analysis, whilst the microstructure was analysed through Mercury Intrusion Porosimetry (MIP) and Scanning Electron Microscopy (SEM).

The XRD patterns were obtained with RICOH D-MAX/2500PC using monochromatic CuKα radiation and running with 2θ in the range of 5^{o}-70^{o} at a speed of 2^{o}/min.

The FTIR spectra were obtained on a Perkin Elmer Spectrum One Spectrometer over the range of 4000cm^{-1} and 400cm^{-1}. Specimens were prepared using the KBr pellet technique through mixing 1 mg of AAFA powder sample with 300 mg of KBr.

The TG analysis was carried out using a TGA/DSC-1600. The samples were heated from 50^{o}C to 1000 ^{o}C at a rate of 10^{o}C/min, during which the oven was purged with N_2 at 100ml/min.

The pore distribution of hardened AAFA samples was investigated by MIP method with an AUTOPore IV 9500 Micromeritics Instrument.

A FEI Quanta200 SEM was used to examine the morphology of the hydration products.

3. RESULTS AND DISCUSSION

3.1 Development of compressive strength

Figure 2 shows the development of compressive strength of AAFA materials with thermal oven curing method. It can be seen that under thermal oven curing, the early-age strength of AAFA was very low at only 2.5 MPa after 2 hours. Prolonged curing time had a positive effect on the development of compressive strength of AAFA under 85^{o}C oven curing condition. There was an approximate 200% increase in compressive strength after 24 hours of thermal oven curing compared to the samples with 4 hours thermal oven curing.

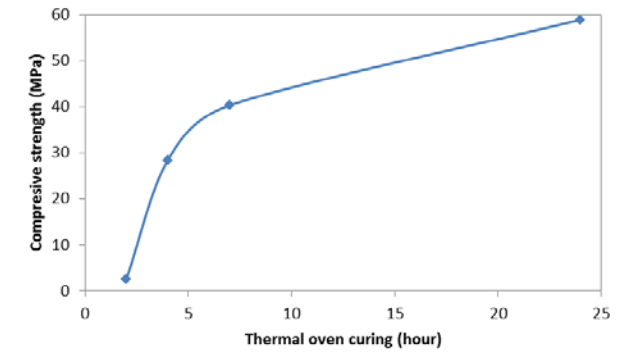

Figure 2. Compressive strength of AAFA under thermal oven curing.

The development of compressive strength of AAFA materials under microwave curing over curing time is shown in Fig. 3. The strength development of the samples with microwave curing method was significantly accelerated compared to the samples cured with thermal oven curing method. The strength of AAFA samples with microwave curing of 20 duty cycles (total power-on time of 2 min) was nearly comparable to those obtained by thermal curing for 7 hours. With longer microwave processing time, the strength of AAFA samples increased. The highest compressive strength of AAFA samples was obtained after 30 duty cycles (48.3 MPa). A slight decrease in the strength can be observed after 40 duty cycles of microwave curing.

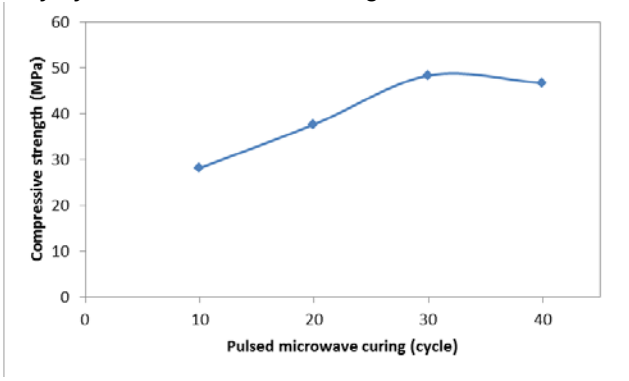

Figure 3. Compressive strength of AAFA under pulsed microwave curing.

3.2 Temperature profiles of AAFA samples under thermal oven curing and microwave curing

Figure 4 shows the temperature profiles of AAFA samples cured at 85^{o}C in a thermal oven for different durations. It can be seen that the temperature distribution was radiant. The highest temperature was always located at the core of the cross-section of AAFA samples. However, the temperature at the core of the sample was below the set temperature of the thermal oven, i.e. 85°C.

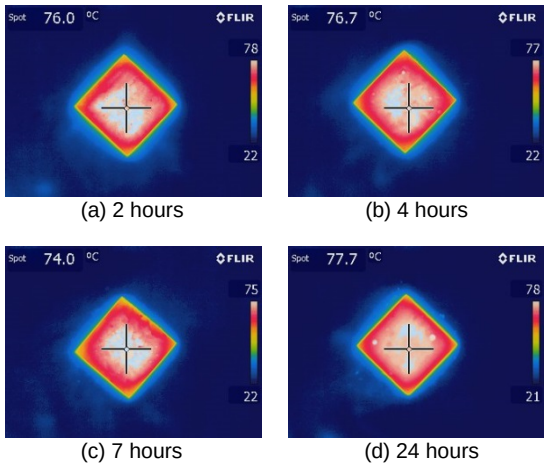

(a) 2 hours (b) 4 hours

(c) 7 hours (d) 24 hours

Figure 4. Thermal images of cross-section of AAFA samples under thermal oven curing.

The thermal images of the cross-section of the AAFA samples under pulsed microwave curing are shown in Fig. 5. It can be observed that all the highest temperatures in the four thermal images were above 100°C.

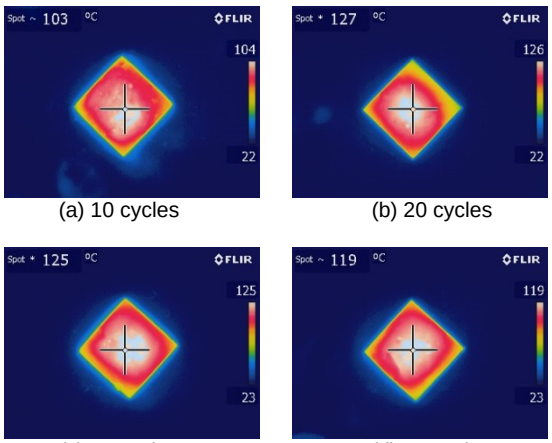

(a) 10 cycles (b) 20 cycles

(c) 30 cycles (d) 40 cycles

Figure 5. Thermal images of cross-section of AAFA samples under pulsed microwave curing.

3.3 Characterization of the reaction products of AAFA with thermal oven curing and pulsed microwave curing

3.3.1 X-ray diffraction (XRD)

Figure 6 presents the XRD spectra of the raw fly ash and AAFA samples under thermal oven curing at 85°C over curing time. It can be seen that the raw fly ash is an amorphous material (as indicated by a halo at 17–33° 2θ) with a series of minor crystalline phases, such as quartz, mullite and hematite. After the alkali activation, the crystalline phases, as detected in the raw fly ash, remained apparently unaltered, while the hump representing amorphous phase decreased, indicating that the amorphous phase in raw fly ash had been consumed during alkali activation process. In addition, new peaks appeared at 13.8° and 24° 2θ which could be attributed to hydroxysodalite (atomic Si/Al ratio = 1). This result was in agreement with the findings reported (Criado et al., 2007a; Bakharev, 2005b).

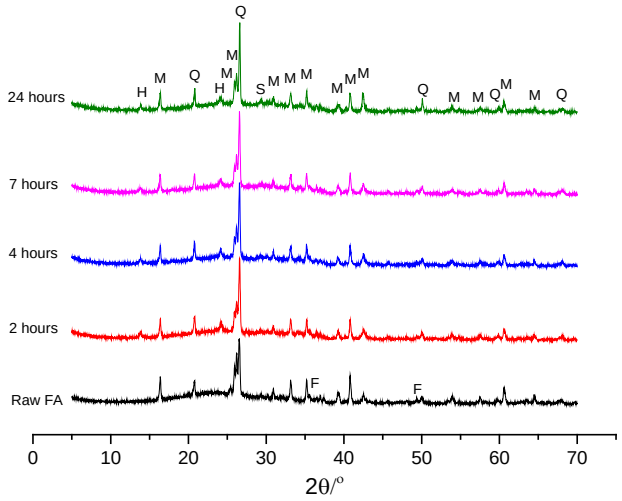

Figure 6. XRD spectra of raw fly ash and AAFA under thermal oven curing (Q-quartz, M-mullite, F-hematite, H-hydroxysodalite, S-sodium silicate).

The XRD patterns of the raw fly ash and AAFA samples with different pulsed microwave curing cycles are presented in Figure 7. Compared to the thermal oven curing, a new crystalline reaction product was identified at 18.0° and 34.2° 2θ, which can be assigned to a zeolite phase, chabazite-Na (atomic Si/Al ratio = 2). These findings are also further interpreted along with the FTIR results below.

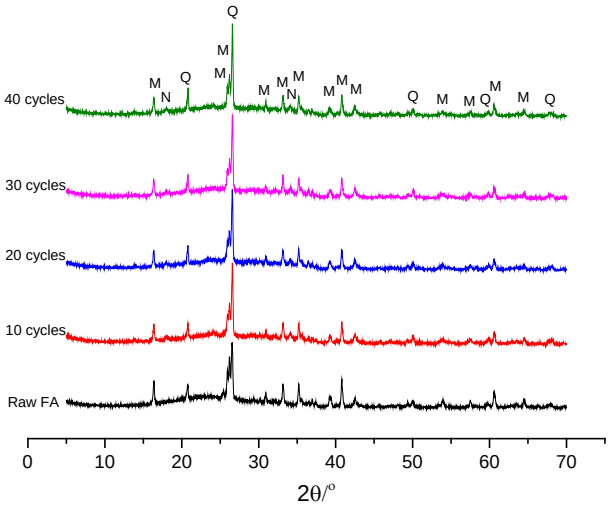

Figure 7. XRD spectra of raw fly ash and AAFA under pulsed microwave curing (Q-quartz, M-mullite, F-hematite, N-chabazite-Na).

3.3.2 Fourier transform infrared spectroscopy (FTIR)

The FTIR spectra of the raw fly ash and two AAFA samples, namely those after, thermal oven curing for 24 hours and pulsed microwave curing for 30 cycles, respectively, were presented in Fig. 8.

The presence of quartz and mullite in the raw fly ash was responsible for the bands at 795 cm^{-1} and 554 cm^{-1} respectively. Both of these two bands barely changed after the activation process, which is consistent with the XRD results, suggesting that the crystalline phases of quartz and mullite are inert and would not take part in the reaction of alkali activation (Fernández-Jiménez & Palomo, 2005). On the other hand, a wide band associated with T-O (T=Al, Si) asymmetric stretching vibrations can be observed in the raw fly ash at 1087 cm^{-1}. After the activation and curing with both thermal oven and microwave oven, this band became sharper and also shifted to lower frequencies 1010 cm^{-1} for thermal oven curing 24 hours and 1007 cm^{-1} for pulsed microwave curing after 30 cycles due to the T-O band vibration of the reaction products in AAFA. This band shift has been regarded as the fingerprint of the formation of alkaline aluminosilicate gel in AAFA [10]. In addition, it can be noticed that this T-O band became sharper and shifted towards lower frequency in the sample of pulsed microwave curing 30 cycles (1007 cm^{-1}) than that in the samples with thermal oven curing for 24 hours (from 1087cm^{-1} to 1007cm^{-1}), implying that the sodium aluminosilicate gel underwent polymerization to a greater extent and its molecular arrangement became more orderly (Criado et al., 2007b). The intensity of the T-O band in the sample under pulse microwave curing for 30 cycles was higher than the one under thermal oven curing for 24 hours, which indicated that pulsed microwave curing could speed up the reaction, resulting in the increase of sodium aluminiumsilicate gel. Moreover, the new bands associated with two new zeolite species appeared around 666 cm^{-1} and 737 cm^{-1} which was interpreted to be the presence of hydroxysodalite (thermal oven curing for 24 hours) and chabazite-Na (pulsed microwave curing 30 cycles) respectively, which was in good agreement with the XRD results reported in the literature (Criado et al., 2005) and in the current study as well. These findings imply that the microwave curing may enhance the transformation process of reaction products from amorphous gel to crystalline zeolite phases, since the Si/Al ratio of chabazite-Na is higher than that of hydroxysodalite.

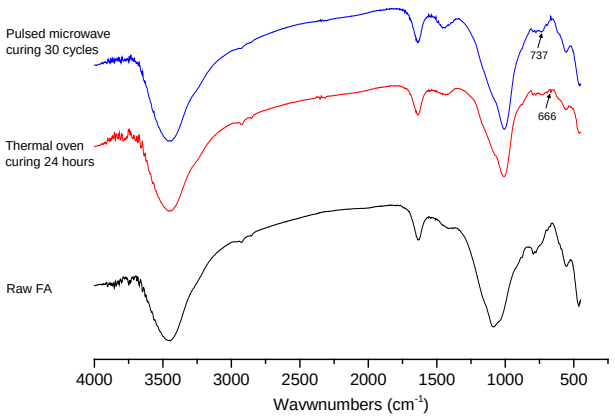

Figure 8. FTIR spectra of raw fly ash and AAFA under thermal oven curing and pulsed microwave curing.

3.3.3 Thermogravimetric and Differential thermogravimetric (TG/DTG) analysis

The TG/DTG curves of the raw fly ash and the AAFAs manufactured under the two different curing regimes are shown in Fig. 9. Again, only two AAFA samples, namely those after, thermal oven curing for 24 hours and pulsed microwave curing for 30 cycles, were selected for the analysis below.

The main weight loss occurred between 100^{o}C to 200°C, (as shown by the strong peak in DTA curves) corresponding to the dehydration of the main reaction products of the two AAFA samples. For the sample under pulsed microwave curing for 30 cycles, the strongest peak was centered around 150°C in the DTG curve, which can be attributed to the sodium aluminosilicate hydrates (Winnefeld et al., 2010). On the other hand, the DTG peak intensity of AAFA under pulsed microwave curing was lower than that under thermal oven curing, implying that aluminosilicate hydrates have undergone higher degree of polymerisation.

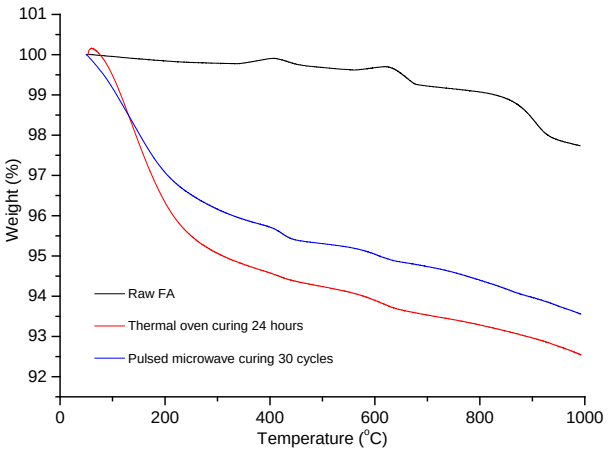

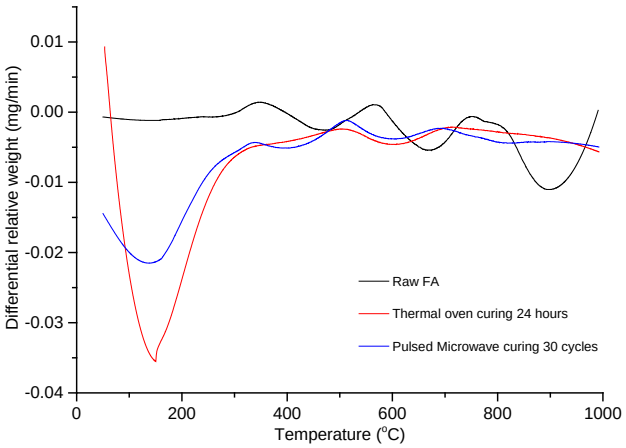

Figure 9. TG/DTG analysis of raw fly ash and AAFA.

3.4 The pore structure and microstructure of AAFA under thermal oven curing and microwave curing

In order to compare the pore structure and microstructure of AAFA produced under different curing methods, again, two samples, namely, the one after thermal oven curing at 85°C for 24 hours and the one after pulsed microwave curing for 30 cycles respectively, were selected and characterized as described below.

3.4.1 Mercury intrusion porosimetry (MIP)

The total porosity of the two AAFA samples under thermal oven curing and pulsed microwave curing is compared in Table 1, while the pore distribution is presented in Fig. 10.

Table 1. Total porosity of AAFA under thermal oven curing and pulsed microwave curing.

Curing method	Total porosity (%)
Thermal oven curing (85°C)	28.51
Pulsed microwave curing	28.12

From Fig.10, it can be seen that in the pore diameter range of 3 μm to 300 μm, the curves of the two samples almost overlap, indicating the amount and the distribution of pores in the pore size range are almost identical. On the other hand, while there exists a considerable amount of the fine pores in the range of 0.1 μm to 0.35 μm in the thermal oven cured AAFA, there are almost no pores that can be identified in the microwave cured AAFA in this region. Furthermore, in the pore size range of 0.35 μm to 3 μm, there are more pores in the microwave cured AAFA compared to the thermal oven cured AAFA. The above results suggest that although microwave curing can promote the early-age strength development, the thermal oven curing can help the formation of denser microstructure.

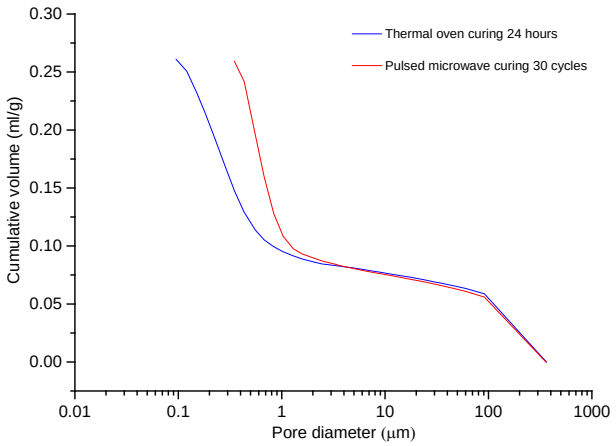

Figure 10. Cumulative pore volume of AAFA under thermal oven curing and pulsed microwave curing.

3.4.2 Scanning electron microscopy (SEM)

Figure 11 presents the fracture surface of the AAFA manufactured with the two different curing methods. Both of these two samples featured heterogeneous microstructure and compacted texture. The reaction products formed on the surface of fly ash particles and in the region between the fly ash particles also can be observed in both samples. It is generally believed that this is due to the formation of this products which contributed to the development of the strength (Rattanadecho et al., 2008). Overall, compared to the microwave cured sample, the thermal oven cured sample demonstrated more compacted microstructure, which corroborates to the results obtained by compressive strength test.

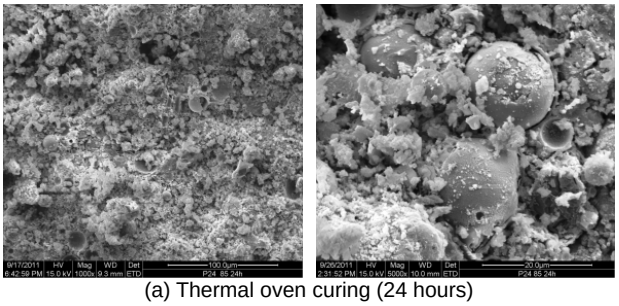

(a) Thermal oven curing (24 hours)

(a) Pulsed microwave curing (30 cycles)

Figure 11. SEM images of AAFA.

3.5 Comparison of energy consumption of AAFA produced by different curing methods

Table 2 shows the energy consumption of AAFA manufactured with different curing methods. As expected, compared to the thermal oven curing, very low energy consumption has been achieved from pulsed microwave curing method.

Table 2. Energy consumption (EC) of AAFA under thermal oven curing and pulsed microwave curing.

Curing method	Duration	Total EC [kJ]	Strength (MPa)	EC [kJ/MPa]
Oven	24 hours	86400	58.9	1147
Microwave	***3 min*** (30 cycles)	***117***	***48.3***	***2.42***

3.6 General discussion

Table 3 compares the main findings from the XRD, FTIR and TG/DTG results.

Table 3. Comparison of reaction products of AAFA.

	Thermal oven curing	Pulsed microwave curing
XRD	Hydroxysodalite Atomic Si/Al ratio=1 (13.8^o 2θ / 24^o 2θ)	Chabazite-Na Atomic Si/Al ratio=2 (18.0^o 2θ / 34.2^o 2θ)
FTIR	Sodium aluminosilicate hydrates ($1010\ cm^{-1}$)	Sodium aluminosilicate hydrates ($1007\ cm^{-1}$)
	Hydroxysodalite ($666\ cm^{-1}$)	Chabazite-Na ($737\ cm^{-1}$)
TG/ DTG	Sodium aluminosilicate hydrates	Sodium aluminosilicate hydrates

It can be seen that based on the XRD study, hydroxysodalite was identified as the main crystalline phase formed in the thermal oven cured AAFA, whilst chabazite-Na was identified as the main crystalline phases formed in the microwave cured AAFA. In addition, the degree of polymerization of aluminosilicate gel in microwave curing samples was higher than that in the thermal oven curing samples.

The obtained results therefore suggest that microwave curing could be an effective method to cure AAFA products with much less curing time than thermal oven curing.

4. CONCLUSIONS

The results presented in this paper demonstrate that the use of microwave sources has great potential to be an alternative curing method for manufacturing AAFA. The compressive strength of AAFA sample manufactured with pulsed microwave curing was comparable with that of thermal oven curing. However, the strength development of the AAFA manufactured with microwave was much faster than that of thermal oven curing. The highest compressive strength was found from the sample under thermal oven curing at 85^oC for 24 hours, which also showed the densest microstructure in the SEM study. The XRD results demonstrated that different reaction products were generated under thermal oven curing (hydroxysodalite) and pulsed microwave curing (chabazite-Na). The FTIR test showed higher degree of polymerization of aluminosilicate product in the microwave cured AAFA. Overall, pulsed microwave curing could help reduce the energy consumption in manufacturing AAFA.

ACKNOWLEDGEMENTS

Miss Shi Shi is sponsored by China Scholarship Council (CSC) for her PhD study at University College London (UCL, UK). Xi'an University of Architecture and Technology (XAUAT, China) and Queen's University Belfast (QUB, UK) provided facilities for this research. The fly ash used in this research was supplied by Weihe coal power plant, Shaanxi, China. The support from the above-mentioned organizations is gratefully acknowledged.

REFERENCES

Bakharev, T. (2005a). Durability of geopolymer materials in sodium and magnesium sulfate solutions. *Cement and Concrete Research, 35,* 1233–1246.

Bakharev, T. (2005b). Geopolymeric materials prepared using Class F fly ash and elevated temperature curing. *Cement and Concrete Research, 35,* 1224–1232.

Criado, M., Fernandez-Jimenez, A., de la Torre, A. G., Aranda, M. A. G., & Palomo, A. (2007a). An XRD study of the effect of the SiO2/Na2O ratio on the alkali activation of fly ash. *Cement and Concrete Research, 37*, 671–679.

Criado, M., Fernandez-Jimenez, A., & Palomo, A. 2007b. Alkali activation of fly ash: Effect of the SiO2/Na2O ratio Part I: FTIR study. *Microporous and Mesoporous Materials, 106***,** 180–191.

Criado, M., Palomo, A., & Fernandez-Jimenez, A. 2005. Alkali activation of fly ashes. Part 1: Effect of curing conditions on the carbonation of the reaction products. Fuel, 84**,** 2048-2054.

Durán-Herrera, A., Juárez, C. A., Valdez, P., & Bentz, D. P. (2011). Evaluation of sustainable high-volume fly ash concretes. *Cement and Concrete Composites, 33*, 39–45.

Felekoglu, B. (2006). Utilisation of Turkish fly ashes in cost effective HVFA concrete production. *Fuel, 85*, 1944–1949.

Fernandez-Jimenez, A., & Palomo, A. (2005). Mid-infrared spectroscopic studies of alkali-activated fly

ash structure. *Microporous and Mesoporous Materials, 86*, 207–214.

Fernandez-Jimenez, A., Palomo, A., & Criado, M. (2005). Microstructure development of alkali-activated fly ash cement: A descriptive model. *Cement and Concrete Research, 35*, 1204–1209.

Fernandez-Jimenez, A., García-Lodeiro, I., & Palomo, A. (2006). Durability of alkali-activated fly ash cementitious materials. *Journal of Materials Science, 42*, 3055–3065.

Fonta, P. 2013. New data for cement industry shows reductions in CO2 emission. *World Cement*.

Gunasekaran, S., & Yang, H. W. (2007a). Effect of experimental parameters on temperature distribution during continuous and pulsed microwave heating. *Journal of Food Engineering, 78*, 1452–1456.

Gunasekaran, S., & Yang, H. W. (2007b). Optimization of pulsed microwave heating. *Journal of Food Engineering, 78*, 1457–1462.

Hutchison, R. G., Chang, J. T., Jennings, H. M., & Brodwin, M. E. (1991). Thermal acceleration of Portland cement mortars with microwave energy. *Cement and Concrete Research, 21*, 795–799.

Katz, A. 1998. Microscopic study of alkali-activated fly ash. *Cement and Concrete Research, 28*, 197–208.

Knoerzer, K., Regier, M., & Schubert, H. (2008). A computational model for calculating temperature distributions in microwave food applications. *Innovative Food Science & Emerging Technologies, 9*, 374–384.

Leung, C. K. Y., & Pheeraphan, T. (1995). Microwave Curing of Portland-Cement Concrete—Experimental Results and Feasibility for Practical Applications. *Construction and Building Materials, 9*, 67–73.

Leung, C. K. Y., & Pheeraphan, T. (1997). Determination of optimal process for microwave curing of concrete. *Cement and Concrete Research, 27*, 463–472.

Ma, Y., Hu, J., & Ye, G. 2012. The effect of activating solution on the mechanical strength, reaction rate, mineralogy, and microstructure of alkali-activated fly ash. *Journal of Materials Science, 47*, 4568–4578.

Makul, N., Rattanadecho, P., & Agrawal, D. K. (2010). Microwave curing at an operating frequency of 2.45 GHz of Portland cement paste at early-stage using a multi-mode cavity: Experimental and numerical analysis on heat transfer characteristics. *International Communications in Heat and Mass Transfer, 37*, 1487–1495.

Metaxas, A. C., & Meredith, R. J. 1983. Industrial microwave heating London: Peregrinus on behalf of the Institution of Electrical Engineers.

Miranda, J. M., Fernandez-Jimenez, A., González, J. A., & Palomo, A. 2005. Corrosion resistance in activated fly ash mortars. *Cement and Concrete Research, 35*, 1210–1217.

Palomo, A., Grutzeck, M. W., & Blanco, M. T. (1999). Alkali-activated fly ashes - A cement for the future. *Cement and Concrete Research, 29*, 1323–1329.

Puertas, F., Amat, T., Fernandez-Jimenez, A. & Vazquez, T. (2003). Mechanical and durable behaviour of alkaline cement mortars reinforced with polypropylene fibres. *Cement and Concrete Research, 33***,** 2031-2036.

Rattanadecho, P., Suwannapum, N., Chatveera, B., Atong, D., & Makul, N. (2008). Development of compressive strength of cement paste under accelerated curing by using a continuous microwave thermal processor. *Materials Science and Engineering, 472*, 299–307.

Somaratna, J., Ravikumar, D. & Neithalath, N. (2010). Response of alkali activated fly ash mortars to microwave curing. *Cement and Concrete Research, 40*, 1688–1696.

Winnefeld, F., Leemann, A., Lucuk, M., Svoboda, P. & Neuroth, M. (2010). Assessment of phase formation in alkali activated low and high calcium fly ashes in building materials. *Construction and Building Materials, 24*, 1086–1093.

Wu, X. Q., Dong, J. G., & Tang, M. S. (1987). Microwave curing technique in concrete manufacture. *Cement and Concrete Research, 17*, 205–210.